FLATNESS BASED OPTIMAL NONCAUSAL OUTPUT-TRANSITIONS FOR CONSTRAINED SISO NONLINEAR SYSTEMS

GL Wang [*,1] **F Allgöwer** [**]

[*] *School of Information Science & Technology*
Sun Yat-Sen University
Guangzhou 510275, China PR
[**] *Institute for System Theory in Engineering*
University of Stuttgart, Pfaffenwaldring 9
D-70550 Stuttgart, Germany

Abstract: The issue of optimal output transition is studied for nonlinear SISO systems with constraints. Trajectory planning is mainly concerned to facilitate exact feedforward linearization in the two-degree-of-freedom design framework. Our approach makes use of the differential parametrization offered by the flatness property. Our contribution to this idea is the generation of a noncausal trajectory for the flat output. This approach is shown to be highly effective in creating performance improvement. It is notable that our methodology guarantees the planned trajectories feasible for all nonlocal transitions. This allows the application of stable inversion in planning the optimal output transitions. The proposed method is illustrated on a benchmark system.

Keywords: Flatness, output transition, constrained nonlinear systems, trajectory planning

1. INTRODUCTION

In this work, we are interested in the issue of the output transition between two (nonlocal) operating points for constrained SISO nonlinear systems. Our study will focus on generating a feedforward input and reference state trajectory while meeting the optimal transition objects under the constraint. This is essential to exact feedforward linearization, which has aroused considerable interest for nonlinear control systems (Hagenmeyer and Delaleau, 2003).

Flatness is a notation originally associated with two kinds of system equivalences: endogenous feedback equivalence (Fliess *et al.*, 1995), and Lie-Bäcklund equivalence (Fliess *et al.*, 1999). More precisely, a flat system is equivalent to a system without dynamics, fully described by the so-called flat output, that has the same dimensionality as the control. For a flat system, there is a one-to-one correspondence between the input-state and a flat output. Of special interest is that the input and state can be expressed as functions of a flat output and its derivatives. A flat output exists in a low-dimensional manifold but still contains all the original information on the system trajectories in a high-dimensional space, thus it leads to the reduction of the system complexity. In particular, a trajectory planning problem is significantly simplified if the trajectories to be followed are designed in flat output coordinates. This property has trigged consierable research activity focused on exploiting the flatness feature in trajectory generation (Rothfuss *et al.*, 1996; Nieuwstadt and Murray, 1998; Oldenburg and Marquardt, 2002). Our contribution to this idea is the generation of a noncausal trajectory in the flat

[1] Partially supported by the Alexander von Humboldt Foundation of Germany and by the NSF of China, PR (Project: 60473120)

output space. This turns out to be highly effective for the performance improvement.

Some methods concerning noncausal output-transitions have been reported in (Piazzi and Visioli, 2001; Perez and Devasia, 2003) for linear systems, where the notation of stable inversion plays an important role. In (Piazzi and Visioli, 2001), the transition time is used to parameterize the real output specified as a polynomial. The transition object with the input and output constraints is optimized with the transition time. In (Perez and Devasia, 2003), stable inversion is employed to establish the parametrization of the planned trajectory and the transition object in terms of the initial and final values of the internal state. Compared with the standard optimal state-transition techniques, the performance improvement can be made by optimizing the transition object with these two parameters. However, it seems to be difficult to extend the above results to nonlinear cases. The main difficulty lies on the fact that the trajectories planned in the real output space are often infeasible for nonlocal transition tasks of nonlinear systems (Perez *et al.*, 2002). The key to our approach is to parameterize the planned trajectory in the flat output space instead of the real output space. This guarantees that the planned trajectory is achievable for all possible transitions. Therefore, our approach augments the applicability of stable inversion in planning the optimal output transitions.

2. OUTLINE OF OUR APPROACH

Consider the nonlinear SISO system

$$\dot{\boldsymbol{x}}(t) = \boldsymbol{f}[\boldsymbol{x}(t), u(t)] \quad \text{(1a)}$$
$$y(t) = h[\boldsymbol{x}(t)] \quad \text{(1b)}$$

with time $t \in \mathbb{R}$, state $\boldsymbol{x} \in \mathbb{R}^n$, input $u \in \mathbb{R}$ and real output $y \in \mathbb{R}$. The vector field $\boldsymbol{f} : \mathbb{R}^n \times \mathbb{R} \to \mathbb{R}^n$ and the function $h : \mathbb{R}^n \to \mathbb{R}$ are real-analytic. We have the following assumptions for the system's output, flatness and equilibria.

A1 The relative degree r of the system (1a) with respect to the output y in (1b) is well-defined and less then n at operating points of interest below.

A2 There exists a flat output $z \in \mathbb{R}$ such that

$$z = F(\boldsymbol{x}) \quad \text{(2a)}$$
$$\boldsymbol{x} = \boldsymbol{\phi}(z, \dot{z}, \cdots, z^{(n-1)}) \quad \text{(2b)}$$
$$u = \psi(z, \dot{z}, \cdots, z^{(n)}) \quad \text{(2c)}$$

where F, $\boldsymbol{\phi}$ and ψ are real-analytic in $\mathbb{R}^n$, $\mathbb{R}^n$ and $\mathbb{R}^{n+1}$, except a finite number of isolated singularities, respectively.

A3 The controllable equilibrium manifold $\mathcal{E}$ defined by $\mathcal{E} = \{(\boldsymbol{x}_e, u_e) | \boldsymbol{f}(\boldsymbol{x}_e, u_e) = 0$, the system (1) is controllable at $\boldsymbol{x}_e\}$ is nonempty.

Obviously, the output set-points of practical interest may be in the set $\mathcal{Y}_e = \{y_e \in \mathbb{R}|$ there exists at least a pair $(\boldsymbol{x}_e, u_e) \in \mathcal{E}$ such that $y_e = h(\boldsymbol{x}_e)$, y_e, $\boldsymbol{x}_e$ and u_e are not singularities for F, $\boldsymbol{\phi}$ and $\psi\}$. Here we are interested in the issue of the output transition between two different (equilibrium) operating points. In particular, it is desired to find a transition trajectory of (1), i.e. the pair $(\boldsymbol{x}, u)$, that the output y is transferred from the present level $\underline{y} \in \mathcal{Y}_e$ at the start time t_s to the new level $\overline{y} \in \mathcal{Y}_e$ at the terminal time $t_f := t_s + \Delta$ while minimizing the transition performance index

$$J(x, u) = \int_{t_s}^{t_f} L[x(t), u(t)]\mathrm{d}t, \quad (3)$$

subject to

$$\boldsymbol{P}[\boldsymbol{x}(t), u(t)] \leq \boldsymbol{0}, \quad (4)$$

where L is a loss cost function, $\Delta \geq 0$ is the transition time, $\boldsymbol{P}$ is an evaluation operator reflecting the physical constraints on the input and state trajectory.

Equations in (2) build up the one-to-one correspondence between the pair $(\boldsymbol{x}, u)$ and the flat output z. This is the basis for our methodology. Let $(\underline{\boldsymbol{x}}, \underline{u})$ and $(\overline{\boldsymbol{x}}, \overline{u})$ be the equilibria in $\mathcal{E}$ corresponding to $\underline{y}$ and $\overline{y}$ in $\mathcal{Y}_e$, respectively. We can determine the corresponding equilibria of the flat output z: $\underline{z}$ and $\overline{z}$ from (2). For every trajectory in the state space for transferring x from $\underline{x}$ to $\overline{x}$, there exists a unique trajectory in the flat output space, along which z is transferred from $\underline{z}$ to $\overline{z}$. Moreover, $\boldsymbol{x}$ and u can be naturally recovered from z without involving the internal dynamics as needed when recovered from y using stable inversion. With this motivation, our approach is to parameterize all admissible transition trajectories in terms of z and its derivatives, from which u and $\boldsymbol{x}$ are determined to meet the optimal transition object.

If the transition effort is limited to the period $[t_s, t_f]$, then the real output transition is equivalent to the flat output transition. That is, $z(t_s) = \underline{z}$ and $z(t_f) = \overline{z}$. Then the remainder freedom is only the generation of $z(\cdot)$ over $[t_s, t_f]$. This leads to the causal feedforward input $u(\cdot)$ and the reference state trajectory $\boldsymbol{x}(\cdot)$ over $[t_s, t_f]$. Planning a trajectory in this way is somewhat conservative and may not be optimal for the output transitions of interest here. Actually, it is not always necessary to constrain $z(t)$ at the initial and final time if the transition effort is distributed over the time domain $\mathbb{R}$ rather than $[t_s, t_f]$. This allows us to seek the solution of the above optimal output transition problem in a much wider range. As a consequence, we are in a position to have an additional freedom of choosing the values of $z(t)$ and derivatives thereof at t_s and t_f in generating the flat output trajectory. This will result in the noncausal feedforward inputs and reference state trajectories. Our approach follow this idea and is outlined as follows.

The idea used here for planning $z(t)$ consists of three primary components: the pre-transition over $I_{pre} = (-\infty, t_s]$, the transition over $I_{tran} = [t_s, t_f]$ and the post-transition over $I_{post} = [t_f, \infty)$. The pre-transition trajectory is generated based on the constraint: for $t \in I_{pre}$,

$$\left.\begin{aligned}\lim_{t\to-\infty} z(t) = \underline{z}\\ h[\boldsymbol{\phi}(z, \dot{z}, \cdots, z^{(n-1)})] = \underline{y}\end{aligned}\right\} \tag{5}$$

That is, along the generated trajectory, $z(t)$ is transferred from the equilibrium point $\underline{z}$ to $z(t_s)$ without changing the output: $y(t) = \underline{y}$ over $t \in I_{pre}$. (5) can be treated as a final value problem thus its bounded solution is acausal. It is clear that freely choosing the values of $z(t)$ and derivatives thereof at t_s offers a freedom to control the shape of the pre-transition trajectory.

Likewise, the post-transition is to generate the trajectory, along which $z(t)$ is driven from $z(t_f)$ to the new equilibrium point $\overline{z}$ without changing the output: $y(t) = \overline{y}$ over $t \in I_{post}$. This can be done based on the constraint: for $t \in I_{post}$,

$$\left.\begin{aligned}\lim_{t\to\infty} z(t) = \overline{z}\\ h[\boldsymbol{\phi}(z, \dot{z}, \cdots, z^{(n-1)})] = \overline{y}\end{aligned}\right\} \tag{6}$$

which can be treated as an initial value problem thus its bounded solution is causal. Clearly, freely choosing the values of $z(t)$ and derivatives thereof at t_f provides a freedom to shape the post-transition trajectory.

Over I_{tran}, we need to generate the trajectory, along which z is transferred from $z(t_s)$ to $z(t_f)$. Clearly, the values of $z(t)$ and derivatives thereof at t_s and t_f and $\Delta = t_f - t_s$ are basic parameters for the transition trajectory. In principle, we can model the transition geometric shape using various spline representations. In our study, a B-spline model is used to represent the transition trajectory $z(t)$ over I_{tran} due to its practical flexibility. The model parameters, which are independent on the basic parameters aforementioned, will be collected as $\mathbf{\Theta}$. In this way, the values of $z(t)$ and derivatives thereof at t_s and t_f, Δ and $\mathbf{\Theta}$ together completely shape $z(t)$ over I_{tran}.

3. PARAMETRIZATION OF FLAT TRAJECTORY

Let z_e denote the equilibrium point of z corresponding to the pair $(\boldsymbol{x}_e, u_e) \in \mathcal{E}$ associated with $y_e \in \mathcal{Y}_e$. The problems posed in (5) and (6) motivate our understanding of the stable transition behavior of $z(t)$ around z_e, subject to

$$h[\boldsymbol{\phi}(z, \dot{z}, \cdots, z^{(n-1)})] = y_e. \tag{7}$$

Indeed, the solution of (7) describes the trajectory, along which $z(t)$ is transferred without changing the real output. From the system inversion point of view, (7) is just the internal dynamics of (1) in terms of the flat output, which is driven by the constant real output y_e. Refer to (Hagenmeyer and Zeitz, 2004), the output y can be parameterized by the flat output z and its first $(n - r)$ derivatives. Let $\boldsymbol{\eta} = [z, \dot{z}, \cdots, z^{(n-r-1)}]^T$. Accordingly, (7) can be written in the form of

$$\dot{\boldsymbol{\eta}} = \boldsymbol{q}(\boldsymbol{\eta}, y_e). \tag{8}$$

with $\boldsymbol{q}(\boldsymbol{\eta}_e, y_e) = \mathbf{0}$, where $\boldsymbol{\eta}_e = [z_e, 0, \cdots, 0]^T$. Let $W^s(\boldsymbol{\eta}_e)$ and $W^u(\boldsymbol{\eta}_e)$ denote the local stable and unstable manifolds at the equilibrium point $\boldsymbol{\eta}_e$, respectively. That is, any points on the stable manifold $W^s(\boldsymbol{\eta}_e)$ will eventually converge to the equilibrium point $\boldsymbol{\eta}_e$ in forward time, and any point on the unstable manifold $W^u(\boldsymbol{\eta}_e)$ will eventually converge to the equilibrium point $\boldsymbol{\eta}_e$ in backward time. Locally $W^s(\boldsymbol{\eta}_e)$ can be defined by an equation $B^s(\boldsymbol{\eta}) = 0$ and, similarly, $W^u(\boldsymbol{\eta}_e)$ can be defined by $B^u(\boldsymbol{\eta}) = 0$. Refer to (Chen and Paden, 1996) for the technical details about the notations of the stable and unstable manifolds.

At this stage, we express the transition relation from $\boldsymbol{\eta}(s)$ to $\boldsymbol{\eta}(t)$ in the form of

$$\boldsymbol{\eta}(t) = \boldsymbol{\eta}(s) + \int_s^t \boldsymbol{q}[\boldsymbol{\eta}(\tau), y_e] d\tau. \tag{9}$$

From the above transition relationship, the following result is followed.

Claim 1. For a trajectory $\boldsymbol{\eta}(t)$ generated by (9)

(i) if $W^u(\boldsymbol{\eta}_e) \neq \{\boldsymbol{\eta}_e\}$ and $B^u(\boldsymbol{\eta}(s)) = 0$, then $\boldsymbol{\eta}(t)$ for $t < s$ is an acausal bounded solution of the the internal dynamics (8) with the final value $\boldsymbol{\eta}(s)$ and $\lim_{t\to-\infty} \boldsymbol{\eta}(t) = \boldsymbol{\eta}_e$;
(ii) if $W^s(\boldsymbol{\eta}_e) \neq \{\boldsymbol{\eta}_e\}$ and $B^s(\boldsymbol{\eta}(s)) = 0$, then $\boldsymbol{\eta}(t)$ for $t > s$ is a causal bounded solution of the internal dyanmics (8) with the initial value $\boldsymbol{\eta}(s)$ and $\lim_{t\to\infty} \boldsymbol{\eta}(t) = \boldsymbol{\eta}_e$.

Now we can discuss the parameterizations of the pre- and post-transition trajectories of $z(t)$.

Pre-transition: Following Claim 1 with $y_e = \underline{y}$ and $\boldsymbol{\eta}_e = \underline{\boldsymbol{\eta}} := [\underline{z}, 0, \cdots, 0]^T$, we arrive at

Claim 2. For the pre-transition trajectory generation, if $W^u(\underline{\boldsymbol{\eta}}) \neq \{\underline{\boldsymbol{\eta}}\}$ and $B^u(\boldsymbol{\eta}(t_s)) = 0$, then the goal of the pre-transition defined in (5) can be fulfilled by

$$\boldsymbol{\eta}(t) = \boldsymbol{\eta}(t_s) + \int_{t_s}^t \boldsymbol{q}[\boldsymbol{\eta}(\tau), \underline{y}] d\tau, \ t \in I_{pre} \tag{10}$$

which leads to an acausal trajectory $z(t)$ parameterized in terms of the values of $z(t)$ and its first $n - r$ derivatives at t_s. Otherwise, the pre-transition trajectory degenerates to the trivial case: $z(t) = \underline{z}$ over I_{pre}.

Post-transition: Again following Claim 1 with $y_e = \overline{y}$ and $\boldsymbol{\eta}_e = \overline{\boldsymbol{\eta}} := [\overline{z}, 0, \cdots, 0]^T$, we have

Claim 3. For the post-transition trajectory generation, if $W^s(\overline{\boldsymbol{\eta}}) \neq \{\overline{\boldsymbol{\eta}}\}$ and $B^s(\boldsymbol{\eta}(t_f)) = 0$, then the goal of the post-transition defined in (6) can be fulfilled by

$$\boldsymbol{\eta}(t) = \boldsymbol{\eta}(t_f) + \int_{t_f}^t \boldsymbol{q}[\boldsymbol{\eta}(\tau), \overline{y}] d\tau, \ t \in I_{post} \tag{11}$$

which leads to a causal trajectory $z(t)$ parameterized in terms of the values of $z(t)$ and its first $n - r$ derivatives at t_f. Otherwise, the post-transition trajectory degenerates to the trivial case: $z(t) = \overline{z}$ over I_{post}.

Transition: The role of the transition trajectory planning over I_{tran} is to fill up the gap between the pre- and post-transition thus piecing them together. The noticeable discontinuities in the input are often unacceptable in practical applications. To avoid this issue, it demands that the planned trajectory for $z(t)$ should be sufficient smoothing. In setting the smooth specification on $z(\cdot)$, we may take the advantage of the following properties drawn from (2c).

Claim 4. $u(\cdot) \in C^{(l)}$ if and only if $z(\cdot) \in C^{(l+n)}$ with l being a nonnegative integer.

Here the notation $C^{(i)}$ denotes the space of the scalar real functions which are continuous till the ith time derivatives. It is followed from (10) and (11) that $z(\cdot)$ are in C^{∞} over both I_{pre} and I_{post}. Thus $u(\cdot) \in C^{(l)}$ if and only if $z(\cdot) \in C^{(l+n)}$ over I_{tran}. Without loss of generality, the generated feedforward input is expect to be continuous. This requires that $z(\cdot) \in C^{(n)}$. In what follows, we will show that $\boldsymbol{\eta}(t_s)$ and $\boldsymbol{\eta}(t_f)$ play a fundamental role in the parametrization of $z(t)$. Thereafter, $\boldsymbol{\eta}(t_s)$ and $\boldsymbol{\eta}(t_f)$ are denoted as $\boldsymbol{\eta}_s$ and $\boldsymbol{\eta}_f$, respectively.

Firstly, we assume that the pre- and post-transition are not trivial. That is, both $W^u(\underline{\boldsymbol{\eta}}) \neq \{\underline{\boldsymbol{\eta}}\}$ and $W^s(\overline{\boldsymbol{\eta}}) \neq \{\overline{\boldsymbol{\eta}}\}$. We can represent $z(t)$ over I_{tran} in the following B-spline form

$$z(t) = \sum_{j=0}^{m} B_{j,p}(t) Z_j,\ t \in I_{tran} \tag{12}$$

where $B_{j,p}$'s are B-spline basis functions of degree p, $\{Z_j\}_{j=0}^{m}$ is the control point set associated with a knot set $I_{knot} = \{t_0, t_1, \cdots, t_{m+p+1}\} \subset I_{tran}$. For simplicity, we generate the knots as follows:

$$t_{j-1} = t_s,\ t_{n+j} = t_f,\ j = 1, 2, \cdots, p+1, \tag{13a}$$
$$t_{p+j} = j\delta_t,\ j = 1, 2, \cdots, m-p, \tag{13b}$$

where $\delta_t = \Delta/(m-p+1)$. Calling for the properties of B-spline(De Boor, 1978), we can parameterize Z_1, Z_2, $\cdots$, Z_n and Z_{m-n}, Z_{m-n+1}, $\cdots$, Z_{m-1} in terms of $(\boldsymbol{\eta}_s, \boldsymbol{\eta}_f, \Delta)$. We collect the remainder control points $Z_j, j = n+1, n+2, \cdots, m-n-1$ into $\boldsymbol{\Theta}$. As a result, we can parameterize $z(t)$ over I_{tran} in terms of $(\boldsymbol{\eta}_s, \boldsymbol{\eta}_f, \Delta, \boldsymbol{\Theta})$. Obviously, $\boldsymbol{\Theta} \neq \emptyset$ if and only if the number of the control points m is larger than $2(n+1)$.

Remark 1. When $W^u(\underline{\boldsymbol{\eta}}) = \{\underline{\boldsymbol{\eta}}\}$, the pre-transition becomes trivial. According to Claim 2, the above trajectory generation needs to be modified by replacing $\boldsymbol{\eta}_s$ by $\underline{\boldsymbol{\eta}}$ and setting $z^{(n-r+1)}(t_s) = \cdots = z^{(n)}(t_s) = 0$. Similarly, if $W^s(\overline{\boldsymbol{\eta}}) = \{\overline{\boldsymbol{\eta}}\}$, referring to Claim 3, we need to replace $\boldsymbol{\eta}_f$ by $\overline{\boldsymbol{\eta}}$ and set $z^{(n-r+1)}(t_f) = \cdots = z^{(n)}(t_f) = 0$. The extreme situation is that both of the pre- and post-transitions are degenerated. This is the case when $W^u(\underline{\boldsymbol{\eta}}) = \{\underline{\boldsymbol{\eta}}\}$ and $W^s(\overline{\boldsymbol{\eta}}) = \{\overline{\boldsymbol{\eta}}\}$. As shown in (Perez *et al.*, 2002), finding a feasible trajectory in the real output space is a challenging issue to fulfill the transition objects in this situation. This is not surprising because the planned trajectory in the real output space generally does not guarantee that the internal state lands on its equilibria at both t_s and t_f, respectively. We emphasize that this difficulty can be avoided by means of the flatness in our approach. Indeed, the above planned trajectory is still feasible even though the above extreme case occurs. Our approach removes the known limitations of planning noncausal transition trajectories in the real output space.

4. OPTIMAL OUTPUT TRANSITION: SIMULATION FOR ICSTR

Let $\boldsymbol{\gamma}$ denote the parameter vector associated with the parametrization of $z(t)$, comprising all or some of $(\boldsymbol{\eta}_s, \boldsymbol{\eta}_f, \Delta, \boldsymbol{\Theta})$. Recall Claim 2 and 3 in the section above that the admissible set of $\boldsymbol{\gamma}$ is characterized by

$$\Gamma = \left\{\boldsymbol{\gamma} | B^u(\boldsymbol{\eta}_s) = \mathbf{0}, B^s(\boldsymbol{\eta}_f) = \mathbf{0}\right\}. \tag{14}$$

Substituting the parametrization of the flat output $z(t)$ into (2b) and (2c) gives the parameterizations of $\boldsymbol{x}(t)$ and $u(t)$ in terms of $\boldsymbol{\gamma}$. Therefore, J in (3) and $\boldsymbol{P}$ in (4) can be represented as the functions of $\boldsymbol{\gamma}$, we write them as $J(\boldsymbol{\gamma})$ and $\boldsymbol{P}(\boldsymbol{\gamma}, t)$, respectively. Then we can formulate the optimal output transition problem as

$$\hat{\boldsymbol{\gamma}} = \arg\min_{\boldsymbol{\gamma} \in \Gamma} J(\boldsymbol{\gamma}) \tag{15}$$

subject to

$$\boldsymbol{P}(\boldsymbol{\gamma}, t) \leq \mathbf{0} \tag{16}$$

which is a static constrained optimization issue and can be easily solved without demand on the complex dynamic optimization techniques.

Simulations are performed with a benchmark system, the Isothermal Continuous Stirred Tank Reactor (ICSTR). The ICSTR considered here assumes a reaction scheme due to Van de Vusse, refer to (Chen *et al.*, 1995) for a detailed explanation. The material and enthalpy balance is a major concern in the ICSTR, which is modeled by

$$\dot{x}_1 = -k_1 x_1 - k_3 x_1^2 + u(c - x_1), \tag{17a}$$
$$\dot{x}_2 = k_1 x_1 - k_2 x_2 + u(-x_2), \tag{17b}$$
$$y = x_2, \tag{17c}$$

where c and x_1 are the concentrations of the input and reactant substance, x_2 the concentration of the output desired product, u is the normalized input flow rate of the reactant substance. The output y reflects the grade of the final product. The parameters k_1, k_2, k_3 and c are positive constants under the isothermal condition.

Under new agile manufacturing paradigms, the demand on output transitions increases because batch sizes will be reduced to meet the product specification change (Perez and Devasia, 2003). Transition loss may occur when the products during the transition do not satisfy specified requirements. The transition object of interest here is to minimize the waste loss produced

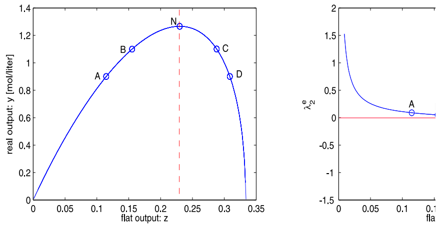

Fig. 1. (left) Operating points; (right) the values of λ_2^e

during the transition. In particular, the transition performance index J is defined by

$$J = \int_{t_s}^{t_f} [y(t)u(t)]\mathrm{d}t, \tag{18}$$

and the constraint $\boldsymbol{P}$ of interest here is specified as

$$u_l \leq u(t) \leq u_r, \tag{19}$$

where $0 < u_l < u_r$ are the constant physical constraints on the control. We define the flat output z as

$$z = x_2/(c - x_1). \tag{20}$$

The expressions of $\boldsymbol{\phi}$ and ψ for the ICSTR are given in Appendix. In this case, $n = 2$ and $r = 1$, thus $\boldsymbol{\eta}$ becomes a scalar, that is, $\eta = z$ and the internal dynamics (7) or (8) becomes

$$\dot{\eta} = \lambda_3^e + (\lambda_2^e - 2\lambda_1^e\eta_e)\eta + \lambda_1^e\eta^2, \tag{21}$$

where λ_1^e, λ_2^e and λ_3^e are given by

$$\lambda_1^e = -k_1 c y_e^{-1} - k_3 c^2 y_e^{-1}, \tag{22a}$$
$$\lambda_2^e = k_1 - k_2 + 2k_3 c + k_1 c y_e^{-1} + 2\eta_e \lambda_1^e, \tag{22b}$$
$$\lambda_3^e = -k_1 - k_3 y_e. \tag{22c}$$

In addition, the solution of (9) for the ICSTR becomes

$$\eta(t) = \eta_e + \frac{\lambda_2^e e^{\lambda_2^e(t-s)}[\eta(s) - \eta_e]}{\lambda_2^e + \lambda_1^e[1 - e^{\lambda_2^e(t-s)}][\eta(s) - \eta_e]}. \tag{23}$$

Clearly, $W^u(\eta_e) \neq \{\eta_e\}$ ($W^u(\eta_e) \neq \{\eta_e\}$) if and only if $\lambda_2^e > 0$ ($\lambda_2^e < 0$). Notice that Γ defined in (14) becomes trivial for the ICSTR.

For comparison purpose, we use the following parameters as in (Perez *et al.*, 2002): $c = 10[\mathtt{mol/L}]$, $k_1 = 50[\mathtt{h}^{-1}]$, $k_2 = 100[\mathtt{h}^{-1}]$, $k_3 = 10[\mathtt{L/(mol.h)}]$. As shown in Figure 1, the operating points in $\mathcal{E}$ are divided into two sets by the dotted line $z = 0.23$, and the values of λ_2^e are positive at the left side and negative at the right side. The output transitions between the operating points 'A','B','C' and 'D' marked in Figure 1 are considered.

In the work of Perez (Perez *et al.*, 2002), the output transitions between the above operation points ware studied, where the output transition trajectory is modelled by a line segment connecting the present and new operating points. There the noncausal trajectory of the internal state, x_1, is parameterized by $x_1(t_s)$, $x_1(t_f)$ and Δ. The optimal parameters were found by minimizing the same waste loss criterion as (18). Here these results will be compared with ours.

In our simulation studies, the B-spline model (12) is used with $p = 4$ and $m = 8$, this guarantees $z(\cdot) \in C^{(2)}$ thus the continuity of $u(\cdot)$. Accordingly, $\boldsymbol{\Theta}$ contains two control points Z_3 and Z_4. As in (Perez *et al.*, 2002), the start transition time is taken as $t_s = 100[\mathtt{sec}]$, the input lower and upper bounds in (4) are taken as: $u_l = 10[\mathtt{L/h}]$ and $u_r = 400[\mathtt{L/h}]$. We list the comparison results in Table 1 and 2, where two important performance indices: the transition time and the waste loss, are involved. The following remarks are in order.

Case 1: Four transition tasks are involved in Case 1, all of them have the well-defined pre- and post-transition trajectories. The first twos correspond to the output transitions that change the internal state but not the output itself. In this case, the problem (15) has trivial solutions $\hat{\gamma}$ characterized by $\hat{\Delta} = 0$ and $\hat{\boldsymbol{\Theta}} = \emptyset$, which leads to $J(\hat{\gamma}) = 0$. The third one in Case 1 corresponds to the transition increasing the output product level and the fourth one vice versa. It can be observed that the waste loss, caused by the transition: 'A' to 'C', is reduced significantly when our approach is applied even though the transition takes a considerable short time. It is interesting to note that transition time for the transition: 'B' to 'D'achieves the minimum values.

Case 2: The two transitions in Case 2 are reverse each other, both the post-transitions are degenerated. Compared with the Perez's, our approach significantly improves the transition performance: the reductions of both the transition time and the waste loss.

Case 3: There are another two reverse transitions in Case 3. Our results are close to the Perez's. It can be observed that the first transition demands on the input maximum level and the second does on the input minimum level over I_{tran}. This is the cost paid for the competitive transition time needed. As shown in Table 2, our approach leads to comparable reductions of the transition time compared with the step-inputs.

Case 4: The four transitions in Case 4 are opposites to those in Case 1. This leads to another extreme situation: both the pre- and post-transition are degenerated. As mentioned in Remark 1, the Perez's approach is not applicable to this case. Indeed, our approach augments the perez's idea in noncausal output transitions by removing the above limitation.

5. CONCLUSIONS

The generation of the feedforward input and the state reference trajectory enables the two-degree-of-freedom design, which offers a framework for the problem of interest: the output transition control of constrained nonlinear systems. This study advocates the flatness based noncausal trajectory generation.

The point that distinguishes our approach from the existing flatness based techniques is the generation of

Table 1. Comparison Results: Case 1 & 2

performance index ↓	transition case →	case 1				case 2	
		A to D	B to C	A to C	B to D	B to A	A to B
transition time [sec]	ours	0	0	16.0	2.44	11.0	47.1
	Perez's	0	0	29.0	2.78	32.4	68.1
	step input	42.8	55	110.3	39.50	59.7	138.6
transition loss [mol/vol]	ours	0	0	0.078	0.240	0.063	0.199
	Perez's	0	0	0.270	0.241	0.337	0.270
	step input	2.759	2.748	0.988	2.728	2.798	0.763

Table 2. Comparison Results: Case 3 & 4

performance index ↓	transition case →	case 3		case 4			
		C to D	D to C	D to A	C to B	C to A	D to B
transition time [sec]	ours	5.07	3.657	142.2	89.1	135.3	96.4
	Perez's	6.87	3.600	NA	NA	NA	NA
	step input	12.2	12.9	195.4	145.9	190.6	151.3
transition loss [mol/vol]	ours	0.524	0.0405	1.584	1.004	1.266	1.255
	Perez's	0.634	0.0390	NA	NA	NA	NA
	step input	0.975	0.6560	1.253	1.700	1.215	1.770

noncausal flat output trajectories. This feature allows us to seek the optimal trajectory in a much wider range thereby benefits the performance improvement. It is notable that our approach guarantees the planned trajectories feasible regardless of the type of the operating points defining a transition task. Our approach removes the known limitations of planning noncausal trajectories in a real output space. This contribution augments the applicability of stable inversion in planning the optimal output transitions.

Our approach is illustrated in the context of the ICSTR, which is a benchmark system for testing nonminimum phase control. Our simulation results demonstrate the effectiveness of our approach.

APPENDIX: THE PARAMETERIZATIONS IN (2) FOR ICSTR

$$\begin{aligned}
\phi_1(z,\dot z) &= [p(z,\dot z)+q(z,\dot z)](2k_3 z)^{-1},\\
\phi_2(z,\dot z) &= [c-\phi_1(z,\dot z)]z,\\
\psi(z,\dot z,\ddot z) &= \left[\frac{\dot z - q(z,\dot z)}{q(z,\dot z)}\right]\left[\frac{k_1\phi_1(z,\dot z)+k_3\phi_1^2(z,\dot z)}{c-\phi_1(z,\dot z)}\right]\\
&\quad -\frac{k_2\dot z+\ddot z}{q(z,\dot z)},
\end{aligned}$$

where $p(z,\dot z)$ and $q(z,\dot z)$ are given by

$$\begin{aligned}
p(z,\dot z) &= -[(k_1-k_2)z-k_1-\dot z],\\
q(z,\dot z) &= \sqrt{[p(z,\dot z)]^2-4k_3cz(k_2z+\dot z)}.
\end{aligned}$$

REFERENCES

Chen, D. and B. Paden (1996). Stable inversion of nonlinear non minimum phase systems. *International Journal of Control* **64**(1), 81–97.

Chen, H., A. Kremling and F. Allgöwer (1995). Nonlinear predictive control of a CSTR benchmark probelm. In: *Proc. of 3rd European Control Conference*. Roma, Italy. pp. 3247–3252.

De Boor, C. (1978). *A Practical Guid to Splines*. Spinger-Verlag.

Fliess, M., J. Lévine, P. Martin and P. Rouchon (1995). Flatness and defect of nonlinear systems: introductory theory and examples. *International Journal of Control* **61**(6), 1327–1361.

Fliess, M., J. Lévine, P. Martin and P. Rouchon (1999). A lie-bäcklund approach to equivalence and flatness of nonlinear systems. *IEEE Transactions on Automatic Control* **44**(5), 922–937.

Hagenmeyer, V. and E. Delaleau (2003). Robustness analysis of exact feedforward linearization based on differential flatness. *Automatica* **39**(11), 1941–1946.

Hagenmeyer, V. and M. Zeitz (2004). Internal dynamics of a nonlinear flat SISO system with respect to a non-flat output. *Systems & Control Letters* **52**(3-4), 323–327.

Nieuwstadt, M. J and R. M. Murray (1998). Real time trajectory generation for differentially flat systems. *International Journal of Robust and nonlinear control*.

Oldenburg, J. and W. Marquardt (2002). Flatness and higher order differential model representations in dynamic optimization. *Computer & Chemical Engineering* **26**, 385–400.

Perez, H. and S. Devasia (2003). Optimal output-transitions for liner systems. *Automatica* **39**(2), 181–192.

Perez, H., B. Oguninaike and S. Devasia (2002). Output tracking between operating points for nonlinear processes: Van de vusse example. *IEEE Transactions on Control Systems Technology* **10**(4), 611–617.

Piazzi, A. and A. Visioli (2001). Optimal noncausal set-point regulation of saclar systems. *Automatica* **37**(1), 121–127.

Rothfuss, R., J. Rudolph and M. Zeitz (1996). Flatness based control of a nonlinear chemical reactor model. *Automatica* **32**(10), 1433–1439.